



Title	I-V measurement of NiO nanoregion during observation by transmission electron microscopy
Author(s)	Fujii, Takashi; Arita, Masashi; Hamada, Kouichi; Kondo, Hirofumi; Kaji, Hiromichi; Takahashi, Yasuo; Moniwa, Masahiro; Fujiwara, Ichiro; Yamaguchi, Takeshi; Aoki, Masaki; Maeno, Yoshinori; Kobayashi, Toshio; Yoshimaru, Masaki
Citation	Journal of Applied Physics, 109(5), 053702 <a href="https://doi.org/10.1063/1.3553868">https://doi.org/10.1063/1.3553868</a>
Issue Date	2011-03-01
Doc URL	<a href="http://hdl.handle.net/2115/45604">http://hdl.handle.net/2115/45604</a>
Rights	Copyright 2011 American Institute of Physics. This article may be downloaded for personal use only. Any other use requires prior permission of the author and the American Institute of Physics. The following article appeared in J. Appl. Phys. 109, 053702 (2011) and may be found at <a href="https://dx.doi.org/10.1063/1.3553868">https://dx.doi.org/10.1063/1.3553868</a>
Type	article
File Information	JAP109-5_053702.pdf



[Instructions for use](#)

## I-V measurement of NiO nanoregion during observation by transmission electron microscopy

Takashi Fujii,<sup>1,a)</sup> Masashi Arita,<sup>1</sup> Kouichi Hamada,<sup>1</sup> Hirofumi Kondo,<sup>1</sup> Hiromichi Kaji,<sup>1</sup> Yasuo Takahashi,<sup>1</sup> Masahiro Moniwa,<sup>2</sup> Ichiro Fujiwara,<sup>2</sup> Takeshi Yamaguchi,<sup>2</sup> Masaki Aoki,<sup>2</sup> Yoshinori Maeno,<sup>2</sup> Toshio Kobayashi,<sup>2</sup> and Masaki Yoshimaru<sup>2</sup>

<sup>1</sup>Graduate School of Information Science and Technology, Hokkaido University, Sapporo 060-0814, Japan

<sup>2</sup>Semiconductor Technology Academic Research Center, 3-17-2 Shinyokohama, Kohoku-ku, Yokohama, 222-003, Japan

(Received 21 October 2010; accepted 7 January 2011; published online 8 March 2011)

Conduction measurements with simultaneous observations by transmission electron microscopy (TEM) were performed on a thin NiO film, which is a candidate material for resistance random access memories (ReRAMs). To conduct nanoscale experiments, a piezo-controlled TEM holder was used, where a fixed NiO sample and a movable Pt-Ir counter electrode were placed. After the counter electrode was moved to make contact with NiO, I-V measurements were carried out from any selected nanoregions. By applying a voltage of 2 V, the insulating NiO film was converted to a low resistance film. This phenomenon may be the “forming process” required to initialize ReRAMs. The corresponding TEM image indicated a structural change in the NiO layer generating a conductive bridge with a width of 30–40 nm. This finding supports the “breakdown” type forming in the so-called “filament model” of operation by ReRAMs. The inhomogeneity of resistance in the NiO film was also investigated. © 2011 American Institute of Physics. [doi:10.1063/1.3553868]

### I. INTRODUCTION

Resistance random access memories (ReRAMs) have actively been investigated in the research field of nonvolatile memories as a candidate for universal memory, because they have the potential of yielding high functionality with a large change in resistance along with high-speed access and non-volatility.<sup>1–5</sup> The resistance of ReRAMs having a metal/insulator/metal capacitor structure is changed by simply applying voltage (e.g., 1–5 V). Of the insulators that have been reported thus far, binary oxides such as NiO, TiO<sub>2</sub>, and CuO (Refs. 4–9) have attracted the most attention because their change in resistance is independent of voltage polarity (unipolar ReRAMs). The most influential mechanism explaining this switching phenomenon may be the “filament model.” Based on this model, a metallike filament is formed at the first application of voltage ( $V_f$ ) within the insulator and connects the metal electrodes.<sup>4–6,9</sup> This process, referred to as “forming” is needed to initialize the ReRAMs. The resistance changes to a low resistance state (LRS) with this forming process. With the second application of voltage  $V_r$  ( $<V_f$ ), the resistance is typically increased much more than ten-fold [high resistance state (HRS)] due to the filament rupturing by oxidation (the “reset” process). Within the third application  $V_s$  ( $V_r < V_s < V_f$ ), the resistance returns to LRS by reduction (a “set” process). After this, the resistance reversibly switches between HRS and LRS by alternating reset and set processes. Although the details of this mechanism have not yet been experimentally confirmed and the switching mechanism is still not understood, the initial

forming process certainly plays a key role in qualifying the properties of ReRAMs.

In order to understand the forming process, it may be useful for us to observe the filament formation. Some studies reported observations of filaments before and after the application of voltage by means of scanning electron microscopy (SEM).<sup>9</sup> Though a single bridge-like path was confirmed, it is necessary to research inside the bridge for observing real-time filament formation. *In situ* transmission electron microscopy (TEM) simultaneously performed with physical (e.g., electrical) measurements<sup>10–12</sup> has attracted a great amount of attention to satisfy this demand. The number of such studies using piezo TEM holders has been increasing in the past few years. For example, the appearance and disappearance of a superstructure in PCMO by application of voltage,<sup>13</sup> obtaining I-V hysteresis of Pr<sub>0.7</sub>Ca<sub>0.3</sub>MnO<sub>3</sub> (PCMO) in TEM,<sup>14</sup> and the observation of a filament-like structure change in TiO<sub>2</sub>.<sup>15</sup>

In this work the above mentioned *in situ* TEM using a piezo-controlled specimen holder was applied to NiO to study the mechanism responsible for the change in resistance, especially that of the forming process. The appearance of a conducting bridge (or filament) was identified in a nanoscale local region of the NiO film.

### II. EXPERIMENTAL

A schematic of the experimental system is shown in Fig. 1(a). The system is composed of a custom-made TEM holder, a control system for the piezo actuator, a current measurement unit, and a CCD camera system.<sup>12,16</sup> The TEM instrument was a JEM 2010 microscope (200 kV, Cs = 0.5 mm), whose vacuum was about  $10^{-5}$  Pa. The TEM holder

<sup>a)</sup>Electronic mail: t-fujii@ist.hokudai.ac.jp.

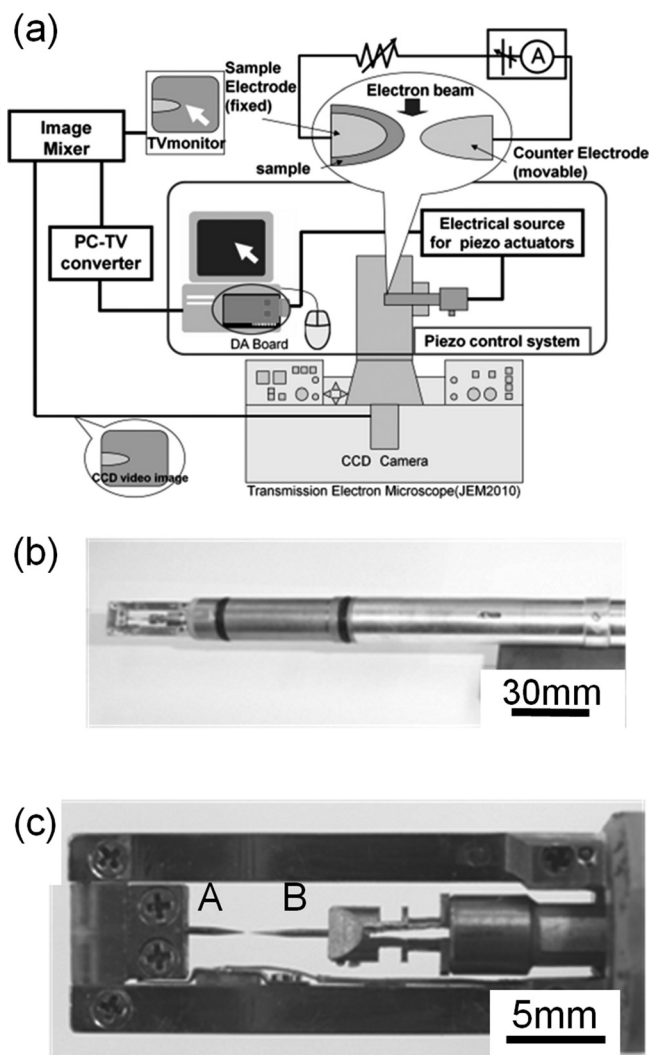


FIG. 1. (a) Schematic of experimental system, (b) TEM specimen holder, and (c) margin of holder where specimens are placed.

used in this work is shown in Figs. 1(b) and 1(c). This holder has three functions. The first is positioning an electrode with sub-nanometer scale accuracy. Two tip-shaped electrodes are placed at A and B as seen in Fig. 1(c). The NiO/Pt-Ir sample is fixed at position A. However, the Pt-Ir counter electrode at B can be moved using software we developed in our laboratory. The second function is measuring the current down to less than nano-amperes. Inside the TEM holder are an electric circuit composed of coaxial cables and a built-in amplifier (gain:  $10^3$ – $10^5$ ). The amplifier can be switched off to measure currents larger than microamperes. The third function is measuring load using a semiconductor sensor on the order of less than *micronewtons*. While this function was not frequently used in this work, mechanical contact between two electrodes could easily be detected.

It has been reported that a NiO layer sandwiched between two Pt electrodes has superior ReRAM properties.<sup>7</sup> Therefore, commercially available Pt-Ir tips for scanning tunneling microscopy (STM) were used as electrodes in this work. One of the electrode tips was covered with a NiO layer and was used as the specimen we investigated. The conduction properties were measured between the Pt-Ir counter

electrode and NiO/Pt-Ir. The TEM images were recorded using a CCD video camera.

To obtain I-V data from the nanoregions, very sharp counter electrodes should be used, whose apex is several tens of nanometers or less. For this purpose, Pt-Ir STM tips were further sharpened using ion milling as well as the ion shadow method.<sup>17</sup> There is a TEM image of a Pt-Ir counter electrode in Fig. 2(a). The apex of the tip-shaped Pt-Ir electrode was about 10 nm or less. The Pt-Ir sample electrode covered with NiO should be wide and thin to enable multiple investigations in one batch. For this purpose, the Pt-Ir tip was mechanically ground into the shape of a wedge. After that, it was polished by conventional ion milling. An example of this is shown in Figs. 2(b) and 2(c). The electrode was about 50  $\mu\text{m}$  wide and thin enough for TEM observations. The Ni was deposited by RF sputtering of a Ni metal target

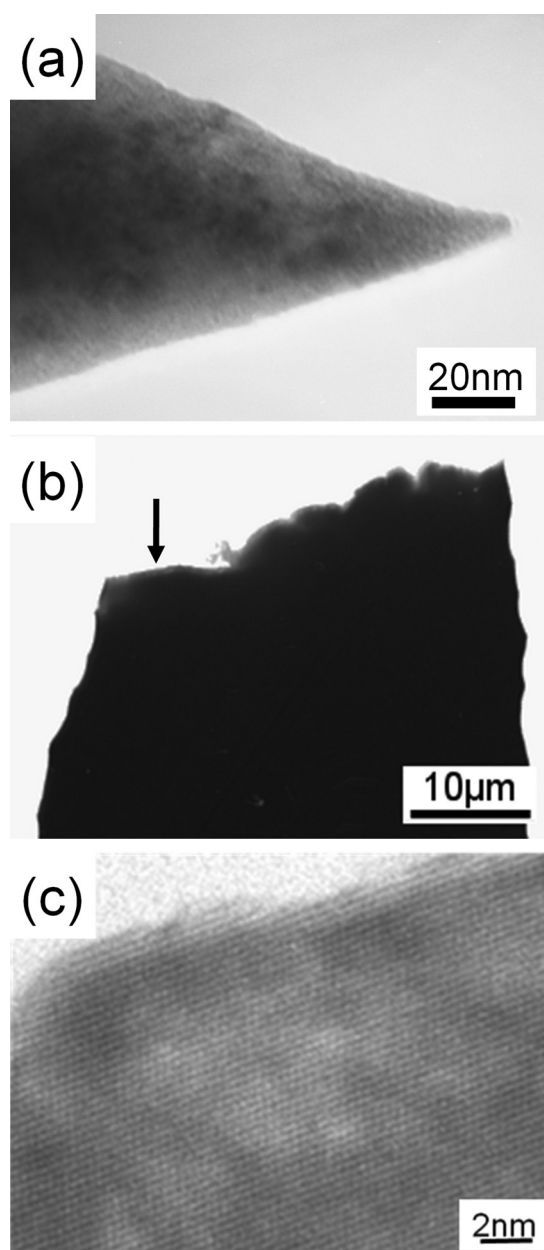


FIG. 2. TEM images of the Pt-Ir (a) counter electrode and (b) substrate for sample deposition. The area indicated by an arrow in (b) is magnified in (c). The substrate was thin enough to observe TEM lattice fringes.

onto this wedge-shaped electrode. The gas flow during sputtering was Ar 20 SCCM and the vacuum was 1.0 Pa. The deposition was performed at room temperature. Then, the Pt-Ir tip covered with Ni was annealed in air (environmental humidity of about 30%) at 200 or 300 °C. The annealing time was three minutes.

### III. RESULTS AND DISCUSSION

Prior to the electrical measurements, the quality of the NiO layer at the top of the wedge-shaped Pt-Ir electrode was checked through conventional TEM observations. The TEM image is shown in Fig. 3. The NiO layer was well crystallized under the preparation conditions described above. A layer having a thickness of about 40–50 nm on the polycrystalline Pt-Ir electrode was composed of polycrystalline NiO grains with an average size of about 30–50 nm. The grain size was inhomogeneous depending on the surface roughness of the Pt-Ir tip. The size of the apex of the Pt-Ir counter electrode was comparable to or less than this grain size, and thus the I-V characteristics could be obtained from individual grains.

A TEM image taken just after the approach of the electrode is shown in Fig. 4(a). The dark upper right region corresponds to the Pt-Ir electrode on which the NiO layer (bright contrast) was deposited. The black region at the bottom left was the Pt-Ir counter electrode. As can be seen from this figure, a sharp Pt-Ir electrode was moved along the direction of the thick arrow to make an electrical connection with the NiO layer. The contact area was about 1200 nm<sup>2</sup> or less, assuming a circular shape. We began to measure the conducting properties of Pt-Ir/NiO/Pt-Ir through this point. The voltage sweep sequence was typically from 0 to +3 V and back to 0 V again. The measurement was done within 18 s in which the drift of the electrode could be neglected. In general, the current is abruptly increased by the forming process and the film is possibly permanently destroyed. To prevent this destruction, a resistor (resistance  $R = 10$  k $\Omega$ ) was inserted in series in the circuit.

The TEM images taken in this process are shown in Fig. 4 and the corresponding I-V curve is shown in Fig. 5.

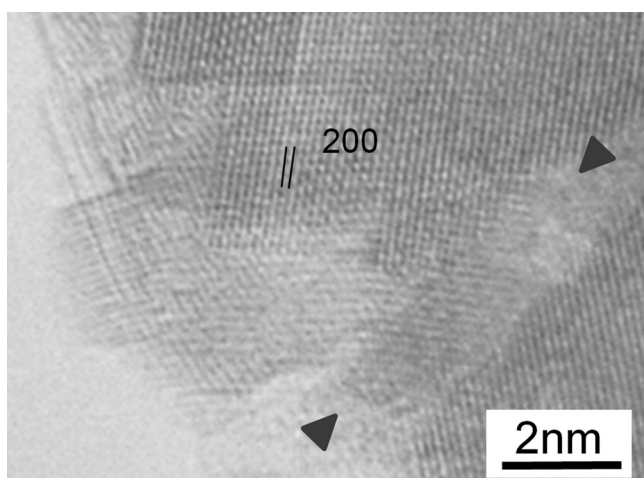


FIG. 3. High resolution TEM image showing NiO lattice fringes. The grain boundary is indicated by arrows. The sample was prepared at 300 °C.

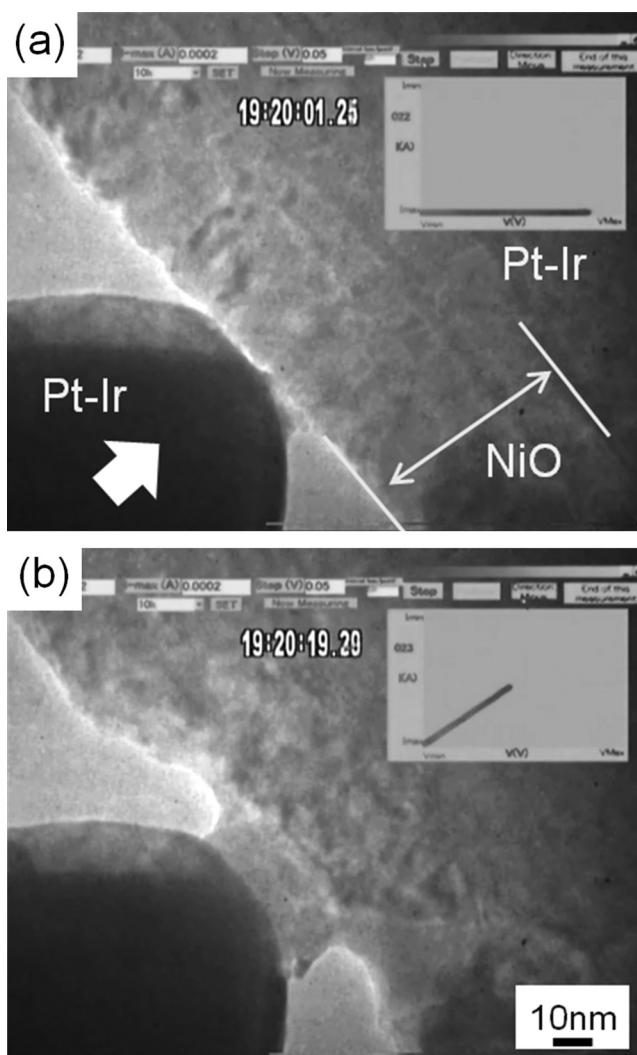


FIG. 4. TEM image of the Pt-Ir counter electrode approaching NiO (a) before and (b) after the conductive bridge is formed. Numbers in the middle at the top represent time (hr: min: sec).

Figures 4(a) and 4(b) correspond to sequences 1 and 2 in Fig. 5. The NiO hardly passed any current in the first sequence, indicating that NiO was originally insulating about 1 M $\Omega$ . When a voltage of 1.7 V was applied, the NiO film

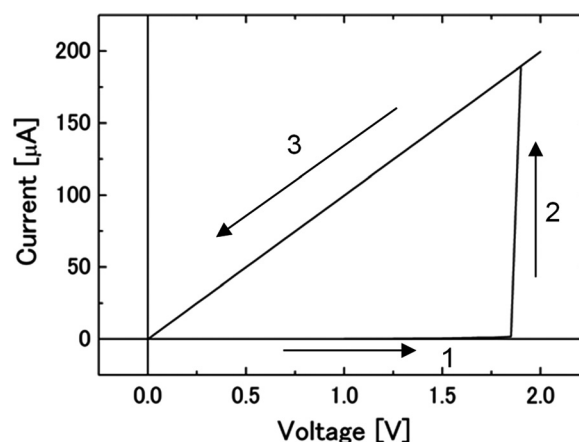


FIG. 5. I-V characteristics measured in TEM corresponding to Fig. 4. Arrows indicate the direction and numbers indicate sequences of cycles.

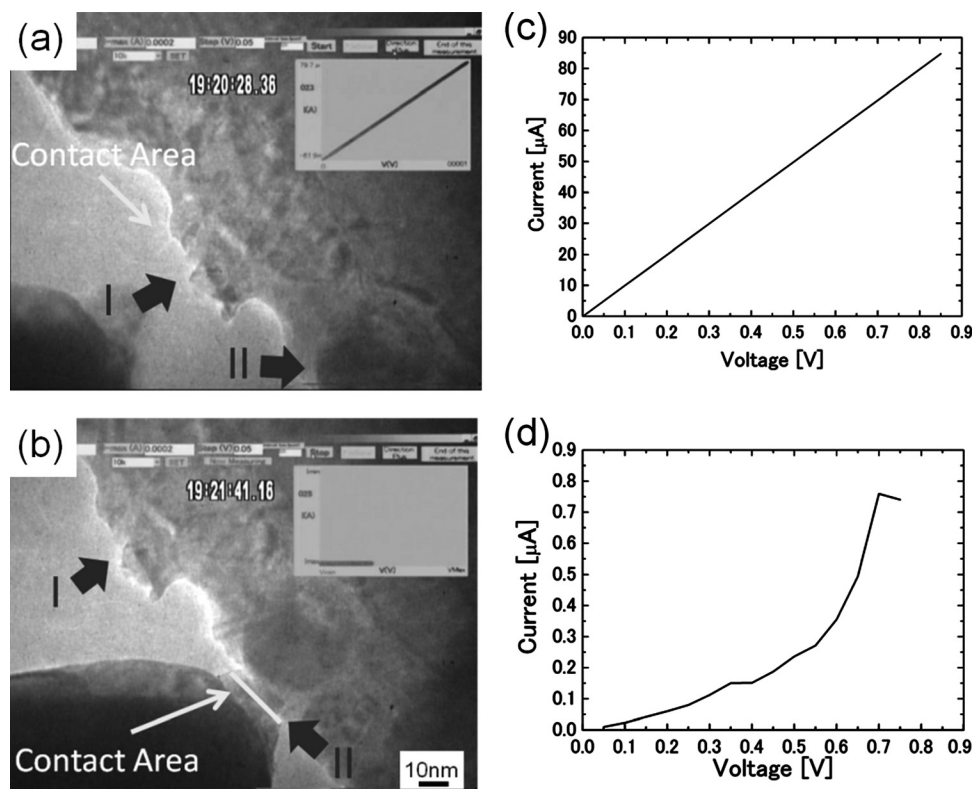


FIG. 6. (a) and (b) TEM image when tip contacts the bridge and the region outside it. Dark thick arrows I and II in these images denote bridge positions that correspond to each other. (c) and (d) I-V characteristics corresponding to images (a) and (b). Note the magnification of the vertical axis in these graphs differs by 100 times.

structure was changed [Fig. 4(b)] and the current suddenly increased (sequence 2 in Fig. 5). When the voltage was decreased from 1.7 to 0 V (sequence 3 in Fig. 5), the I-V curve was almost that of  $R = 10 \text{ k}\Omega$ , i.e., the resistance inserted in series. The NiO resistance had been changed to LRS ( $R \ll 10 \text{ k}\Omega$ ). When the measurement ended the Pt-Ir electrode was detached from NiO/Pt-Ir and again approached the same position I, as shown in Fig. 6(a). The resistance was still in LRS [Fig. 6(c)]. We call this area a *bridge*. The width of the bridge was 45 nm as seen in Fig. 4(b). However, when we approached the adjacent nanoregion II in Fig. 6(b), it remained insulating [Fig. 6(d)]. The I-V curve in Fig. 5 is quite similar to that of the data during the forming process for Pt/NiO/Pt devices measured in air,<sup>7</sup> while the switching voltage and current are slightly different. Therefore, the bridge observed in this work is thought to be a conductive filament used in the operation of ReRAMs. However, alternative reset-set switching was not achieved by sweeping the voltage in this work. The region surrounding the bridge is strongly deformed in Fig. 4(b) probably due to joule heating during the forming process.<sup>18</sup> The oxygen in NiO might continually disperse into the vacuum as has been suggested by earlier work.<sup>9,19</sup> Based on this assumption, the filament is hardly ruptured by oxidation in TEM. This may be why the filament could not be reset in the present work. The results presented here support the model where breakdown contributes to the appearance of a conductive filament during the forming process.<sup>20-22</sup>

Conductive filaments would be generated selectively at weak points against the electric field during the forming process. Therefore, investigations into electric inhomogeneity are important to enable reliable ReRAM devices to be fabricated.

The local conduction properties of NiO films were studied, as seen in Fig. 7. The sample was oxidized at low temperature ( $200^\circ\text{C}$ ) to clearly detect weak points. Figure 7(a) is a TEM image of NiO film containing a grain boundary (see the dashed line). The Pt-Ir electrode made contact at the grain boundary. The corresponding I-V characteristics in Fig. 7(b) were almost those of the resistor inserted in series into the measurement system. The resistance of the film at the grain boundary was low ( $\ll 10 \text{ k}\Omega$ ) and did not change even with higher voltages up to 2.5 V. The Pt-Ir electrode in Fig. 7(c) made contact at the middle of the grain, while avoiding the grain boundaries. The resistance was high enough (about  $2.0 \text{ M}\Omega$ ), and the forming process was accomplished by applying a higher voltage (1.0 V). Although all measurements were not performed under the same condition because of the accidental difference in contact area, a percentage of successful forming was estimated to be about 20% in NiO oxidized at  $200^\circ\text{C}$ . The forming voltage was between 1.0 and 2.5 V. The degree of oxidation must increase by increasing the oxidation temperature and NiO, both at the grain boundary and in the grain, must be well insulating. Even in such cases the grain boundary is the weakest point, and thus the conduction filament is thought to be formed selectively here. Further studies are needed to clarify the origin of the weaknesses in the formation of filaments in NiO ReRAMs.

#### IV. CONCLUSION

The process of forming ReRAMs [Pt-Ir/NiO(50-nm-thick)/Pt-Ir test devices] was investigated by means of *in situ* TEM using a piezo-controlled specimen holder with simultaneous I-V measurements. Starting from the initial state, the resistance abruptly decreased at about 2 V. At the same time, a

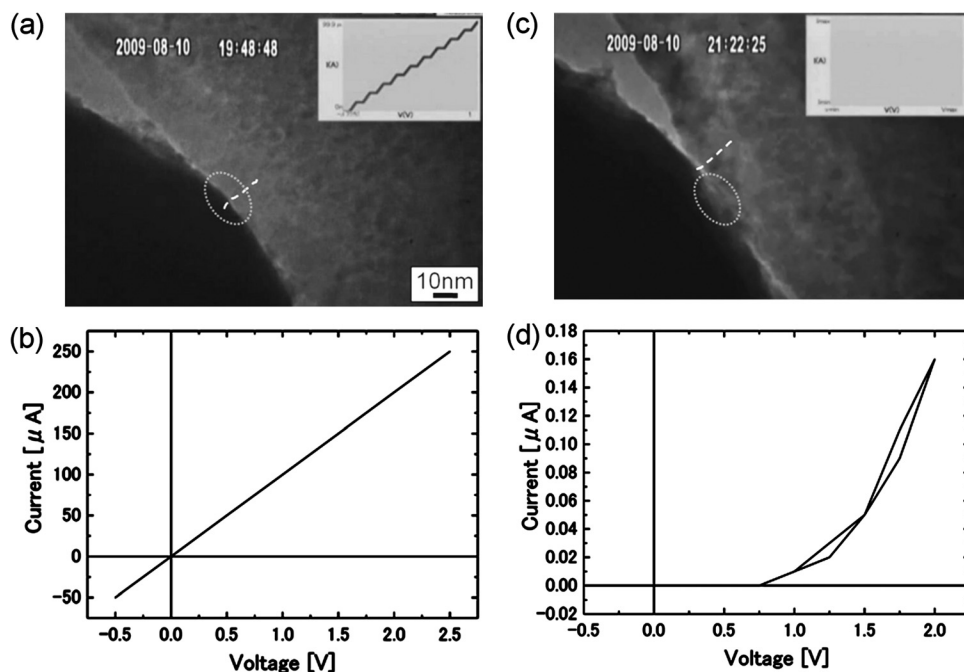


FIG. 7. (a) and (b) TEM image of tip contacting the grain boundary (dashed line) and corresponding I-V data. (c) and (d) TEM image of tip contacting the middle of the grain, and corresponding I-V data. Dotted ellipses in (a) and (c) denote contact regions.

bridge with a width of 40–50 nm was formed. This bridge was very conductive while the surrounding region demonstrated insulating properties. The resistivity of the region at the grain boundary was relatively low and the bridge may have appeared selectively in the grain boundary region. Alternative reset and set phenomena have not presently been attained with the TEM apparatus. For a more detailed discussion on the mechanism responsible for the operation of ReRAMs, we need to confirm reversible switching during TEM observation and find the composition of the bridge.

## ACKNOWLEDGMENTS

This research was partially supported by a grant made available by the Global COE Program, “Center for Next-Generation Information Technology Based on Knowledge Discovery and Knowledge Federation,” from the Ministry of Education, Culture, Sports, Science and Technology of Japan (MEXT). Part of this work was financially aided by MEXT and the Japan Society for the Promotion of Science (JSPS) (Grant Nos. 20035001 and 21560681).

<sup>1</sup>S. Q. Liu, N. J. Wu, and A. Ignatiev, *Appl. Phys. Lett.* **76**, 2749 (2000).

<sup>2</sup>A. Sawa, T. Fujii, M. Kawasaki, and Y. Tokuda, *Appl. Phys. Lett.* **85**, 4073 (2004).

<sup>3</sup>H. Kaji, H. Kondo, T. Fujii, M. Arita, and Y. Takahashi, *IOP Conf. Ser. Mater. Sci. and Eng.* **8**, 012032 (2010).

<sup>4</sup>I. G. Baek, *Tech. Dig. Int. Electron Devices Meet.* 587 (2004).

<sup>5</sup>A. Sawa, *Mater. Today*, **11**, 28 (2008).

<sup>6</sup>G.-S. Park, X.-S. Li, D.-C. Kim, R.-J. Jung, M.-J. Lee, and S. Seo, *Appl. Phys. Lett.* **91**, 222103 (2007).

<sup>7</sup>H. Kondo, H. Kaji, T. Fujii, K. Hamada, M. Arita, and Y. Takahashi, *IOP Conf. Ser. Mater. Sci. and Eng.* **8**, 012034 (2010).

<sup>8</sup>C. Yoshida, K. Tsunoda, H. Noshiro, and Y. Sugiyama, *Appl. Phys. Lett.* **91**, 223510 (2007).

<sup>9</sup>K. Fujiwara, T. Nemoto, M. J. Rozenberg, Y. Nakamura, and H. Takagi, *Jpn. J. Appl. Phys.* **47**, 6266 (2008).

<sup>10</sup>H. Ohnishi, Y. Kondo, and K. Takayanagi, *Nature (London)* **395**, 780 (1998).

<sup>11</sup>T. Kizuka, S. Umehara, and S. Fujiwara, *Jpn. J. Appl. Phys., Part 2* **40**, L71 (2001).

<sup>12</sup>M. Arita, Y. Okubo, K. Hamada, Y. Takahashi, *Superlattices Microstruct.* **44**, 633 (2008).

<sup>13</sup>Ch. Jooss, J. Hoffmann, J. Fladerer, M. Ehrhardt, T. Beetz, L. Wu, and Y. Zhu, *Phys. Rev. B* **77**, 132409 (2008).

<sup>14</sup>T. Fujii, H. Kaji, H. Kondo, K. Hamada, M. Arita, and Y. Takahashi, *IOP Conf. Ser. Mater. Sci. and Eng.* **8**, 012033 (2010).

<sup>15</sup>D.-H. Kwon, K. M. Kim, J. H. Jang, J. M. Jeon, M. H. Lee, G. H. Kim, X.-S. Li, G.-S. Park, B. Lee, S. Han, M. Kim, and C. S. Hwang, *Nature Nanotech.* **5**, 148 (2010).

<sup>16</sup>R. Hirose, M. Arita, K. Hamada, Y. Takahashi, and A. Subagyo, *Jpn. J. Appl. Phys.* **44**, L790 (2005).

<sup>17</sup>R. Hirose, M. Arita, K. Hamada, and A. Okada, *Mater. Sci. Eng., C* **23**, 927 (2003).

<sup>18</sup>D. Ielmini, C. Cagli, and F. Nardi, *Appl. Phys. Lett.* **94**, 063511 (2009).

<sup>19</sup>R. Yasuhara, K. Fujiwara, K. Horiba, H. Kumigashira, M. Kotsugi, M. Oshima, and H. Takagi, *Appl. Phys. Lett.* **95**, 012110 (2009).

<sup>20</sup>K. Kinoshita, T. Tamaru, M. Aoki, Y. Sugiyama, and H. Tanaka, *Appl. Phys. Lett.* **89**, 103509 (2006).

<sup>21</sup>K. M. Kim, B. J. Choi, and C. S. Hwang, *Appl. Phys. Lett.* **90**, 242906 (2007).

<sup>22</sup>C. Cagli, D. Ielmini, F. Nardi, and A. L. Lacaita, *IEDM Tech. Dig.* 308 (2008).